

Surface plasmon polariton analogues of volume electromagnetic wave effects

Felix Huerkamp, Tamara A. Leskova, and Alexei A. Maradudin

Department of Physics and Astronomy
and Institute for Surface and Interface Science
University of California, Irvine CA 92697, U.S.A.

ABSTRACT

We present our recent theoretical studies of surface plasmon polariton analogues of the Goos–Hänchen effect and of Young’s double-slit experiment.

1. INTRODUCTION

In recent years analogues of optical effects originally associated with volume electromagnetic waves have begun to be studied in the context of surface plasmon polaritons. These include negative refraction,^{1,2} the Talbot effect,^{3,4} cloaking,⁵ lasing,^{6,7} and Young’s double-slit experiment.⁸ In this paper we present our recent studies of some of these effects for surface structures that differ from those considered in Refs.^{1,8} and by different approaches as well, and present treatments of some new effects. The effects we consider here are surface plasmon polariton analogues of the Goos–Hänchen effect and of Young’s double-slit experiment. A discussion of the results obtained, and the conclusions that can be drawn from them, ends this paper.

2. THE GOOS–HÄNCHEN EFFECT

When an electromagnetic beam of finite cross section is incident from an optically more dense medium on its planar interface with an optically less dense medium, and the polar angle of incidence is greater than the critical angle for total internal reflection, the reflected beam undergoes a lateral displacement along the interface, as if it has been reflected from a plane in the optically less dense medium parallel to the physical interface. This lateral displacement of the reflected beam is the Goos–Hänchen effect.⁹

In this section we show that a surface plasmon polariton beam can display a Goos–Hänchen effect.

The system we consider consists of vacuum in the region $x_3 > 0$. The region $x_1 < 0, x_3 < 0$ is filled with a metal whose dielectric function is $\epsilon_1(\omega)$, while the region $x_1 > 0, x_3 < 0$ is filled with a metal whose dielectric function is $\epsilon_2(\omega)$ (Fig. 1). The planar interface $x_3 = 0$ between vacuum and each of the metals supports a surface plasmon polariton of frequency ω .

We assume initially that a surface plasmon polariton of this frequency is incident from the region $x_1 < 0$ on the interface $x_1 = 0$ between the two metals. We determine the electromagnetic field of the surface plasmon polariton

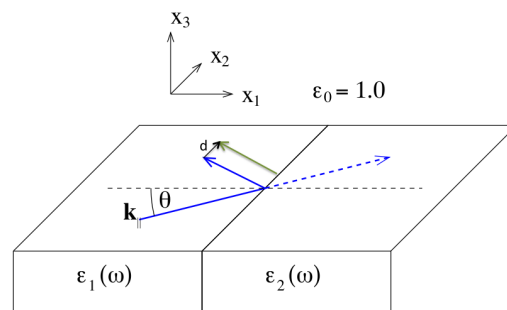


Figure 2.1. The structure studied in Section 2.

reflected from this interface back into the region $x_1 < 0$ by the use of an impedance boundary condition¹⁰ on the surface $x_3 = 0$. We write this boundary condition in the form ($i, j = 1, 2$)

$$J_E(\mathbf{x}_{\parallel}|\omega)_i = K_{ij}^{(0)}(\mathbf{x}_{\parallel}|\omega)J_H(\mathbf{x}_{\parallel}|\omega)_j, \quad (2.1)$$

where $\mathbf{x}_{\parallel} = (x_1, x_2, 0)$ and summation over repeated subscripts is assumed. The vectors $\mathbf{J}_E(\mathbf{x}_{\parallel}|\omega)$ and $\mathbf{J}_H(\mathbf{x}_{\parallel}|\omega)$ are defined by $\mathbf{J}_E(\mathbf{x}_{\parallel}|\omega) = \hat{\mathbf{x}}_3 \times \mathbf{E}^>(\mathbf{x}|\omega)|_{x_3=0}$ and $\mathbf{J}_H(\mathbf{x}_{\parallel}|\omega) = \hat{\mathbf{x}}_3 \times \mathbf{H}^>(\mathbf{x}|\omega)|_{x_3=0}$, where $\mathbf{E}^>(\mathbf{x}|\omega)$ ($\mathbf{H}^>(\mathbf{x}|\omega)$) is the total electric (magnetic) field in the vacuum region $x_3 > 0$, and a caret over a vector denotes a unit vector. The only nonzero elements of the surface impedance tensor $\overset{\leftrightarrow}{K}^{(0)}(\mathbf{x}_{\parallel}|\omega)$ are

$$\begin{aligned} K_{12}^{(0)}(\mathbf{x}_{\parallel}|\omega) &= \kappa_1(\omega) + [\kappa_2(\omega) - \kappa_1(\omega)]S(\mathbf{x}_{\parallel}), \\ &= -K_{21}^{(0)}(\mathbf{x}_{\parallel}|\omega), \end{aligned} \quad (2.2)$$

where

$$S(\mathbf{x}_{\parallel}) = \theta(x_1), \quad (2.3)$$

$\theta(x)$ is the Heaviside unit step function, and $\kappa_j(\omega) = i/(-\epsilon_j(\omega))^{\frac{1}{2}}$.

The total electric field in the vacuum $\mathbf{E}^>(\mathbf{x}|\omega)$ can be written as

$$\begin{aligned} \mathbf{E}^>(\mathbf{x}|\omega) &= \hat{\mathbf{e}}_p^>(\mathbf{k}_{\parallel}) \exp[i\mathbf{k}_{\parallel}(\omega) \cdot \mathbf{x}_{\parallel} - \beta_0(k_{\parallel})x_3] \\ &+ \int \frac{d^2q_{\parallel}}{(2\pi)^2} \exp[i\mathbf{q}_{\parallel} \cdot \mathbf{x}_{\parallel} - \beta_0(q_{\parallel})x_3] \left\{ \hat{\mathbf{e}}_p^>(\mathbf{q}_{\parallel}) \frac{A_{\parallel}^>(\mathbf{q}_{\parallel})}{\beta_0(q_{\parallel}) + i(\omega/c)\kappa_1(\omega)} + \hat{\mathbf{e}}_s^>(\mathbf{q}_{\parallel}) \frac{A_{\perp}^>(\mathbf{q}_{\parallel})}{(\omega/c) - i\kappa_1(\omega)\beta_0(q_{\parallel})} \right\}, \end{aligned} \quad (2.4)$$

where

$$\hat{\mathbf{e}}_p^>(\mathbf{q}_{\parallel}) = (c/\omega) [i\hat{\mathbf{q}}_{\parallel}\beta_0(q_{\parallel}) - \hat{\mathbf{x}}_3q_{\parallel}], \quad (2.5a)$$

$$\hat{\mathbf{e}}_s^>(\mathbf{q}_{\parallel}) = (\hat{\mathbf{x}}_3 \times \hat{\mathbf{q}}_{\parallel}), \quad (2.5b)$$

and $\beta_0(q_{\parallel}) = [q_{\parallel}^2 - (\omega/c)^2]^{\frac{1}{2}}$, with $Re\beta_0(q_{\parallel}) > 0$, $Im\beta_0(q_{\parallel}) < 0$. A time dependence $\exp(-i\omega t)$ has been assumed for this field, but has not been indicated explicitly. The coefficients $A_{\parallel}(\mathbf{q}_{\parallel})$ and $A_{\perp}(\mathbf{q}_{\parallel})$ are the amplitudes of the p - and s -polarized components of the scattered field with respect to the plane of scattering defined by the vectors $\hat{\mathbf{q}}_{\parallel}$ and $\hat{\mathbf{x}}_3$.

The first term on the right-hand side of each of Eqs. (2.4) gives the field of the incident surface plasmon polariton. The vector $\mathbf{k}_{\parallel}(\omega)$ is given by $\mathbf{k}_{\parallel}(\omega) = k_{\parallel}(\omega) (\cos\theta, \sin\theta, 0)$, where $k_{\parallel}(\omega) = (\omega/c)[1 - 1/\epsilon_1(\omega)]^{\frac{1}{2}}$ is the wavenumber of the surface plasmon polariton of frequency ω , in the impedance approximation, at the planar interface between vacuum and a metal whose dielectric function is $\epsilon_1(\omega)$. It is the solution of the dispersion relation

$$\beta_0(k_{\parallel}(\omega)) + i(\omega/c)\kappa_1(\omega) = 0. \quad (2.6)$$

The angle θ is its angle of incidence, measured counterclockwise from the negative x_1 axis, and the function $\beta_0(\omega)$ is $\beta_0(k_{\parallel}(\omega)) = (\omega/c)(-\epsilon_1(\omega))^{-\frac{1}{2}}$.

The magnetic field $\mathbf{H}^>(\mathbf{x}|\omega)$ is obtained from Eq. (2.4) with the use of the relation $\mathbf{H}^>(\mathbf{x}|\omega) = -i(c/\omega)\nabla \times \mathbf{E}^>(\mathbf{x}|\omega)$.

When the expressions for $\mathbf{E}^>(\mathbf{x}|\omega)$ and $\mathbf{H}^>(\mathbf{x}|\omega)$ are substituted into Eqs. (2.1) and (2.2), we obtain a pair of coupled integral equations for the scattering amplitudes $A_{\parallel}(\mathbf{q}_{\parallel})$ and $A_{\perp}(\mathbf{q}_{\parallel})$ that can be written in the forms

$$A_{\parallel}(\mathbf{p}_{\parallel}) + i\frac{\omega}{c}[\kappa_2(\omega) - \kappa_1(\omega)] \int \frac{d^2q_{\parallel}}{(2\pi)^2} \hat{S}(\mathbf{p}_{\parallel} - \mathbf{q}_{\parallel}) \left\{ (\hat{\mathbf{p}}_{\parallel} \cdot \hat{\mathbf{q}}_{\parallel}) \frac{A_{\parallel}(\mathbf{q}_{\parallel})}{\beta_0(q_{\parallel}) + i(\omega/c)\kappa_1(\omega)} - i(\hat{\mathbf{p}}_{\parallel} \times \hat{\mathbf{q}}_{\parallel})_3 \frac{c}{\omega} \beta_0(q_{\parallel}) \frac{A_{\perp}(\mathbf{q}_{\parallel})}{(\omega/c) - i\kappa_1(\omega)\beta_0(q_{\parallel})} \right\} = -i\frac{\omega}{c}[\kappa_2(\omega) - \kappa_1(\omega)] \hat{S}(\mathbf{p}_{\parallel} - \mathbf{k}_{\parallel}) (\hat{\mathbf{p}}_{\parallel} \cdot \hat{\mathbf{k}}_{\parallel}) \quad (2.7a)$$

$$A_{\perp}(\mathbf{p}_{\parallel}) - \frac{\omega}{c}[\kappa_2(\omega) - \kappa_1(\omega)] \int \frac{d^2q_{\parallel}}{(2\pi)^2} \hat{S}(\mathbf{p}_{\parallel} - \mathbf{q}_{\parallel}) \left\{ (\hat{\mathbf{p}}_{\parallel} \times \hat{\mathbf{q}}_{\parallel})_3 \frac{A_{\parallel}(\mathbf{q}_{\parallel})}{\beta_0(q_{\parallel}) + i(\omega/c)\kappa_1(\omega)} + i(\hat{\mathbf{p}}_{\parallel} \cdot \hat{\mathbf{q}}_{\parallel}) \frac{c}{\omega} \beta_0(q_{\parallel}) \frac{A_{\perp}(\mathbf{q}_{\parallel})}{(\omega/c) - i\kappa_1(\omega)\beta_0(q_{\parallel})} \right\} = \frac{\omega}{c}[\kappa_2(\omega) - \kappa_1(\omega)] \hat{S}(\mathbf{p}_{\parallel} - \mathbf{k}_{\parallel}) (\hat{\mathbf{p}}_{\parallel} \times \hat{\mathbf{k}}_{\parallel})_3, \quad (2.7b)$$

where

$$\hat{S}(\mathbf{Q}_{\parallel}) = \int d^2x_{\parallel} S(\mathbf{x}_{\parallel}) \exp(-i\mathbf{Q}_{\parallel} \cdot \mathbf{x}_{\parallel}). \quad (2.8)$$

For the function $S(\mathbf{x}_{\parallel})$ given by Eq. (2.3) we have

$$\hat{S}(\mathbf{Q}_{\parallel}) = \frac{2\pi\delta(Q_2)}{i(Q_1 - i\eta)}, \quad (2.9)$$

where η is a positive infinitesimal.

The translational invariance of our system in the x_2 direction requires that the amplitudes $A_{\parallel,\perp}(\mathbf{q}_{\parallel})$ have the forms

$$A_{\parallel,\perp}(\mathbf{q}_{\parallel}) = 2\pi\delta(q_2 - k_2) a_{\parallel,\perp}(q_1). \quad (2.10)$$

The amplitudes $a_{\parallel,\perp}(q_1)$ satisfy the equations

$$a_{\parallel}(p_1) + i\frac{\omega}{c}[\kappa_2(\omega) - \kappa_1(\omega)] \int_{-\infty}^{\infty} \frac{dq_1}{2\pi i} \frac{1}{p_1 - q_1 - i\eta} \left\{ (\hat{\mathbf{p}}_{\parallel} \cdot \hat{\mathbf{q}}_{\parallel}) \frac{a_{\parallel}(q_1)}{\beta_0(q_{\parallel}) + i(\omega/c)\kappa_1(\omega)} - i(\hat{\mathbf{p}}_{\parallel} \times \hat{\mathbf{q}}_{\parallel})_3 \frac{c}{\omega} \beta_0(q_{\parallel}) \frac{a_{\perp}(q_1)}{(\omega/c) - i\kappa_1(\omega)\beta_0(q_{\parallel})} \right\} = -i\frac{\omega}{c}[\kappa_2(\omega) - \kappa_1(\omega)] \frac{(\hat{\mathbf{p}}_{\parallel} \cdot \hat{\mathbf{k}}_{\parallel})}{i(p_1 - k_1 - i\eta)} \quad (2.11a)$$

$$a_{\perp}(p_1) - \frac{\omega}{c}[\kappa_2(\omega) - \kappa_1(\omega)] \int_{-\infty}^{\infty} \frac{dq_1}{2\pi i} \frac{1}{p_1 - q_1 - i\eta} \left\{ (\hat{\mathbf{p}}_{\parallel} \times \hat{\mathbf{q}}_{\parallel})_3 \frac{a_{\parallel}(q_1)}{\beta_0(q_{\parallel}) + i(\omega/c)\kappa_1(\omega)} + i(\hat{\mathbf{p}}_{\parallel} \cdot \hat{\mathbf{q}}_{\parallel}) \frac{c}{\omega} \beta_0(q_{\parallel}) \frac{a_{\perp}(q_1)}{(\omega/c) - i\kappa_1(\omega)\beta_0(q_{\parallel})} \right\} = \frac{\omega}{c}[\kappa_2(\omega) - \kappa_1(\omega)] \frac{(\hat{\mathbf{p}}_{\parallel} \times \hat{\mathbf{k}}_{\parallel})_3}{i(p_1 - k_1 - i\eta)}. \quad (2.11b)$$

In writing Eqs. (2.11) we have simplified the notation by using the vectors \mathbf{p}_{\parallel} , \mathbf{q}_{\parallel} , and \mathbf{k}_{\parallel} . However, it must

be noted that the 2 component of each of these vectors is now k_2 , so that $\mathbf{p}_{\parallel} = (p_1, k_2, 0)$, $\mathbf{q}_{\parallel} = (q_1, k_2, 0)$, and $\mathbf{k}_{\parallel} = (k_1, k_2, 0)$. Therefore $q_{\parallel} = (q_1^2 + k_2^2)^{\frac{1}{2}}$ in these equations.

The pair of equations (2.11) was solved numerically. The infinite range of integration was replaced by the finite range $(-q_{\infty}, q_{\infty})$. The resulting integrals were converted into sums by the use of an N -point extended midpoint method. The variable p_1 was given the values of the abscissas used in the evaluation of the integrals. A square $2N \times 2N$ supermatrix equation for the values of $a_{\parallel}(q_1)$ and $a_{\perp}(q_1)$ at the values of these abscissas was produced, which was solved by a standard linear equation solver algorithm. The convergence of the solution was monitored by increasing q_{∞} and N systematically until the solution did not change upon further increases of these parameters.

The surface plasmon polariton reflected from the interface $x_1 = 0$ back into the region $x_1 < 0$ of the surface $x_3 = 0$ is p polarized. The p -polarized component of the electric field scattered into the vacuum region $x_3 > 0$ is given by the first term in the integral on the right-hand side of Eq. (2.4). With the use of Eqs. (2.10) this field can be written as

$$\begin{aligned} \mathbf{E}^>(\mathbf{x}|\omega)_{sc,p-pol} &= \frac{c}{\omega} \int_{-\infty}^{\infty} \frac{dq_1}{2\pi} \left[i\beta_0(q_{\parallel})\hat{q}_1, i\beta_0(q_{\parallel})\hat{k}_2, -q_{\parallel} \right] \\ &\times \frac{a_{\parallel}(q_1)}{\beta_0(q_{\parallel}) + i(\omega/c)\kappa_1(\omega)} \exp[iq_1x_1 + ik_2x_2 - \beta_0(q_{\parallel})x_3]. \end{aligned} \quad (2.12)$$

We are still using the convention that the 2 component of each vector is k_2 . The contribution to the field (2.12) from the reflected surface plasmon polariton is given by the residue of the integrand at the simple poles it has when $\beta_0(\sqrt{q_1^2 + k_2^2}) + i(\omega/c)\kappa_1(\omega) = 0$. In fact, the solutions of this equation are $q_1 = \pm k_1(\omega)$, where $k_1(\omega)$ is the 1 component of the vector $\mathbf{k}_{\parallel}(\omega)$. Since we are interested in this field in the region $x_1 < 0$, we need the residue at the pole that lies in the lower half of the complex q_1 plane, namely $q_1 = -k_1(\omega)$. (We assume that $\epsilon_1(\omega)$ has an infinitesimal positive imaginary part to aid this determination.) It can be shown that $a_{\parallel}(q_1)$ has no pole in the lower half of the complex q_1 plane. On evaluating the residue at this pole we obtain for the electric field of the reflected surface plasmon polariton in the region $x_1 < 0$, $x_3 > 0$

$$\mathbf{E}^>(\mathbf{x}|\omega)_{ref,spp} = r(k_1, \omega) \frac{c}{\omega} [-i\beta_0(\omega)\hat{k}_1, i\beta_0(\omega)\hat{k}_2, -k_{\parallel}] \exp[-ik_1x_1 + ik_2x_2 - \beta_0(\omega)x_3], \quad (2.13a)$$

where the reflection amplitude $r(k_1, \omega)$ is

$$r(k_1, \omega) = \frac{\omega}{c} \kappa_1(\omega) \frac{a_{\parallel}(-k_1)}{k_1}. \quad (2.13b)$$

The critical angle θ_c for total internal reflection of a surface plasmon polariton incident from the region $x_1 < 0$ ($\epsilon_1(\omega)$) on the interface $x_1 = 0$ is obtained from the condition $k_2(\omega) = k_{\parallel}(\omega) \sin \theta_c = p_{\parallel}(\omega)$, where $p_{\parallel}(\omega) = (\omega/c)[1 - 1/\epsilon_2(\omega)]^{\frac{1}{2}}$ is the wavenumber, in the impedance approximation, of the surface plasmon polariton of frequency ω at the planar interface between vacuum and a metal whose dielectric function is $\epsilon_2(\omega)$. Thus we find that

$$\sin \theta_c = \frac{p_{\parallel}(\omega)}{k_{\parallel}(\omega)}. \quad (2.14)$$

The existence of this angle clearly requires that $p_{\parallel}(\omega) < k_{\parallel}(\omega)$ or, equivalently, that $|\epsilon_1(\omega)| < |\epsilon_2(\omega)|$ (recall that $\epsilon_j(\omega)$, $j = 1, 2$, must be negative in order that the corresponding surface plasmon polariton exist).

The result given by Eq. (2.13a) has been obtained on the basis of the assumption that the incident surface plasmon polariton has the form of an evanescent plane wave whose angle of incidence measured counterclockwise from the negative x_1 axis is θ . However, observation of the Goos-Hänchen effect requires that the incident surface plasmon polariton have the form of a beam of finite width in the plane $x_3 = 0$. The reflected surface

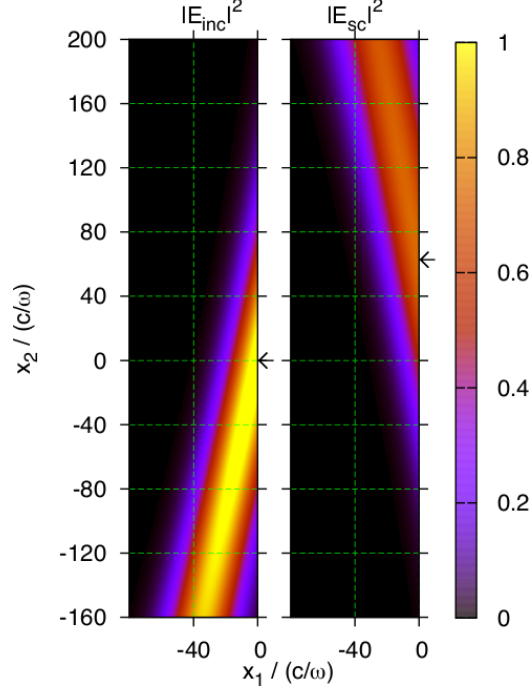


Figure 2.2. (a) A color-level plot of the intensity distribution of a surface plasmon polariton beam incident at an angle of $\theta_0 = 78^\circ$ from a gold surface on its interface $x_1 = 0$ with an aluminum surface. (b) A color-level plot of the intensity distribution of a surface plasmon polariton beam reflected from the interface $x_1 = 0$ of a gold surface with an aluminum surface. The horizontal arrows indicate the position of the maximum intensity of each beam along the interface $x_1 = 0$.

plasmon polariton will then also have the form of a beam of finite width in the plane $x_3 = 0$. To obtain such an incident and scattered field we calculate the right-hand side of Eq. (2.13a) as a function of θ for $-\pi/2 \leq \theta \leq \pi/2$, multiply the result by $(k_{\parallel} w / 2\sqrt{\pi}) \exp[-(k_{\parallel} w / 2)^2 (\theta - \theta_0)^2]$, and integrate the product with respect to θ in the interval $-\pi/2 \leq \theta \leq \pi/2$. In the limit that $(k_{\parallel} w / 2) \gg 1$, the resulting incident surface plasmon polariton has the form

$$\begin{aligned} \mathcal{E}^>(\mathbf{x}|\omega)_{inc,spp} &\cong \frac{c}{\omega} [i\beta_0(\omega) \cos \theta_0, i\beta_0(\omega) \sin \theta_0, -k_{\parallel}] \exp [ik_{\parallel}(x_1 \cos \theta_0 + x_2 \sin \theta_0)] \exp[-\beta_0(\omega)x_3] \\ &\times \exp \left[-\frac{(-x_1 \sin \theta_0 + x_2 \cos \theta_0)^2}{w^2} \right], \end{aligned} \quad (2.15)$$

which is recognized as the electric field of an incident surface plasmon polariton Gaussian beam whose angle of incidence measured counterclockwise from the negative x_1 axis is θ_0 , and whose $1/e$ half width in the direction normal to its direction of propagation is w . The electric field of the reflected surface plasmon polariton is

$$\begin{aligned} \mathcal{E}^>(\mathbf{x}|\omega)_{ref,spp} &\cong \int_{-\pi/2}^{\pi/2} d\theta \frac{k_{\parallel} w}{2\sqrt{\pi}} \exp \left[-\left(\frac{k_{\parallel} w}{2} \right)^2 (\theta - \theta_0)^2 \right] r(k_{\parallel} \cos \theta, \omega) \frac{c}{\omega} [-i\beta_0(\omega) \cos \theta, i\beta_0(\omega) \sin \theta, -k_{\parallel}] \\ &\times \exp [ik_{\parallel}(-x_1 \cos \theta + x_2 \sin \theta) - \beta_0(\omega)x_3], \end{aligned} \quad (2.16)$$

an integral that we evaluate numerically.

We now turn to some results obtained by means of the preceding analysis.

We assume that the region $x_1 < 0$, $x_3 < 0$ is gold, while the region $x_1 > 0$, $x_3 < 0$ is aluminum. A surface plasmon polariton beam of $1/e$ halfwidth w is incident from the region $x_1 < 0$ on the interface $x_1 = 0$. Its

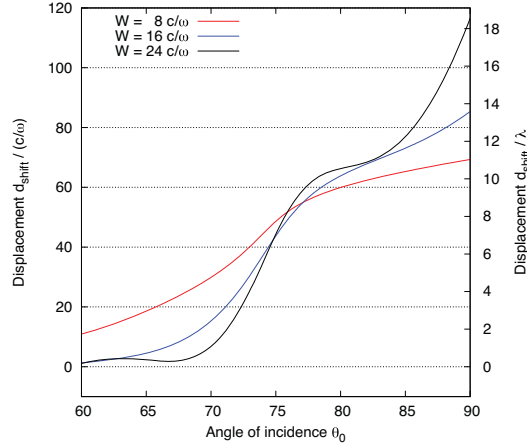


Figure 2.3. The lateral displacement of the reflected surface plasmon polariton beam as a function of the angle of incidence θ_0 for several values of the $1/e$ half width of the incident surface plasmon polariton beam.

frequency ω corresponds to a vacuum wavelength of $\lambda = 632.8$ nm. The dielectric function of gold at that frequency is $\epsilon_1(\omega) = -11.82$, while the dielectric function of aluminum at this frequency is $\epsilon_2(\omega) = -64.07$. The critical angle for total internal reflection in this case is $\theta_c = 75.39^\circ$.

In Fig. 2.2(a) we present a color-level plot of the intensity distribution in the region $x_1 < 0$ and $x_3 = 0.1(c/\omega)$ of the incident surface plasmon polariton beam, whose $1/e$ half width is $w = 16(c/\omega)$, and whose angle of incidence is $\theta_0 = 78^\circ$. In Fig. 2.2(b) we present a color-level plot of the intensity distribution in the region $x_1 < 0$ and $x_3 = 0.1(c/\omega)$ of the reflected surface plasmon polariton beam. The horizontal arrows in these two figures indicate the position of the center of each beam along the interface $x_1 = 0$ between the two metals. It is seen that the reflected beam has its center displaced in the positive x_2 direction from the center of the incident beam by a distance $d_{shift} \cong 61(c/\omega)$.

In Fig. 2.3 we plot the lateral shift of the reflected beam as a function of the angle of incidence θ_0 for three different values of the $1/e$ half width w of the incident surface plasmon polariton beam. The system for which these results were calculated is the same as the one for which Fig. 2.2 was obtained. It is seen that a lateral displacement of the reflected beam occurs even when the angle of incidence θ_0 is smaller than the critical angle for total internal reflection $\theta_c = 75.39^\circ$. This is due to the fact that the incident beam is a superposition of plane waves with a Gaussian distribution of their angles of incidence centered at θ_0 . Because of the finite width of this beam, even if θ_0 is smaller than θ_c some portion of it is a superposition of plane waves whose angles of incidence are greater than θ_c , and it is this portion that produces the lateral shift of the reflected beam. This shift decreases as θ_0 decreases from θ_c because the portion of the incident beam formed from the plane waves whose angles of incidence exceed θ_c decreases rapidly due to the Gaussian distribution of the angles of incidence.

The lateral shifts of the reflected surface plasmon polariton beam calculated here for the gold–aluminum interface appear to be large enough to be observable.

3. YOUNG’S DOUBLE-SLIT EXPERIMENT

The interference fringes observed by Thomas Young¹¹ in the intensity distribution of light transmitted through a pair of nearby pinholes in an opaque screen was the first experimental evidence for the wave nature of light. The same kind of interference pattern is also obtained when the pinholes of Young’s experiment are replaced by narrow slits.¹²

In recent theoretical and experimental work Zia and Brongersma⁸ have studied the surface plasmon polariton analogue of Young’s double slit experiment. In their experiment the slits were represented by two metal stripe waveguides that protruded from an extended metal film region called the launchpad, and terminated at another metal film region called the termination pad. This metal structure was deposited on a glass substrate. A

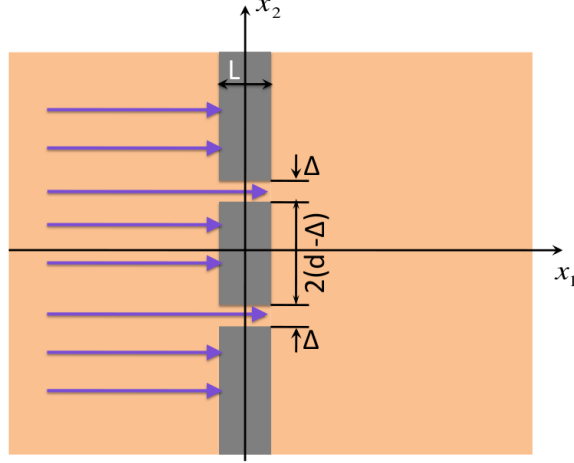


Figure 3.1. The structure studied in Section 3.

photon scanning tunneling microscope (PSTM) was used to determine the local field intensity under its tip in the termination pad. The distribution of this intensity closely resembled the diffraction and interference pattern of Young's double-slit experiment, and was in good agreement with theoretical results obtained by means of the authors' dielectric waveguide model.¹³

In this section we reconsider the theory of the surface plasmon polariton analogue of Young's double-slit experiment. Our approach is based on the impedance boundary condition used in Section 2.

The structure we study consists of vacuum in the region $x_3 > 0$. The region $x_3 < 0$ is filled with a metal whose dielectric function is $\epsilon_1(\omega)$, except in the regions $|x_1| < L/2$, $|x_2| > d$, and $|x_1| < L/2$, $|x_2| < d - \Delta$, which are filled with a dielectric whose (real, positive) dielectric constant is $\epsilon_2(\omega)$ (Fig. 3.1). Note that these portions of the surface $x_3 = 0$ do not support surface plasmon polaritons. Thus the regions $|x_1| < L/2$, $d - \Delta < |x_2| < d$ are slits of length L and width Δ on the surface $x_3 = 0$.

We assume that a surface plasmon polariton of frequency ω in the form of a plane wave is incident on the slits from the region $x_1 < -L/2$ on the surface $x_3 = 0$. Our interest is in the surface plasmon polariton transmitted into the region $x_1 > L/2$ of this surface.

We calculate the transmission of the incident surface plasmon polariton on the basis of the impedance boundary condition (2.1)-(2.2), where now

$$S(\mathbf{x}_{\parallel}) = \theta(L/2 - |x_1|) [\theta(|x_2| - d) + \theta(d - \Delta - |x_2|)]. \quad (3.1)$$

The total electric field in the vacuum is again given by Eq. (2.4), and the amplitudes $A_{\parallel}(\mathbf{q}_{\parallel})$ and $A_{\perp}(\mathbf{q}_{\parallel})$ again satisfy Eqs. (2.7), where now

$$\hat{S}(\mathbf{Q}_{\parallel}) = 2L \text{sinc}(Q_1 L/2) [\pi \delta(Q_2) - d \text{sinc}(Q_2 d) + (d - \Delta) \text{sinc}(Q_2 (d - \Delta))], \quad (3.2)$$

where $\text{sinc}x = \sin x/x$.

Equations (2.7) together with Eq. (3.2) were solved numerically by a two-dimensional extension of the method described in Section 2.

The contribution to the electric component of the scattered field in the vacuum region from the surface plasmon polariton in the region $x_1 > L/2$ is given by the residue at the pole of the first term in the integrand

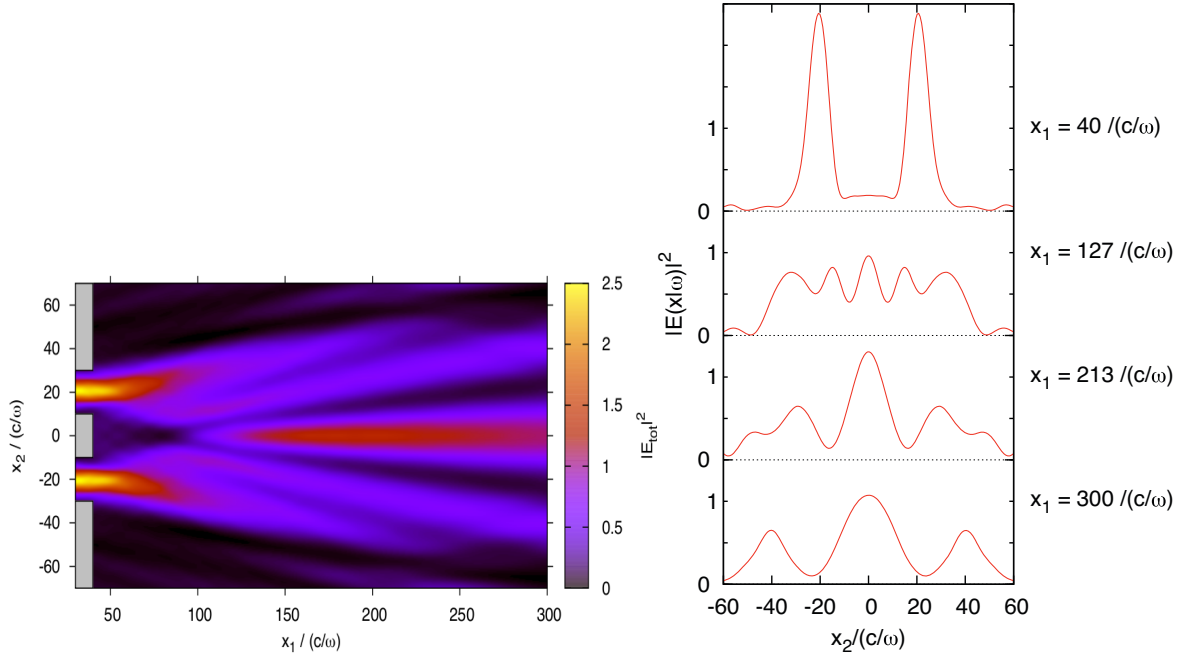


Figure 3.2. (a) A color-level plot of the intensity distribution of the surface plasmon polaritons transmitted through a pair of slits as a function of the distance from the exits of the slits. (b) Lateral cross sections of the intensity distribution at increasing distances from the exits of the slits.

on the right-hand side of Eq. (2.4) at $q_{\parallel} = k_{\parallel}(\omega)$. It can be written in the form

$$\begin{aligned} \mathbf{E}^>(\mathbf{x}|\omega)_{tr,spp} &= \exp[-\beta_0(\omega)x_3] \int_{-\pi/2}^{\pi/2} \frac{d\phi_q}{2\pi} \exp[ik_{\parallel}(\omega)x_{\parallel} \cos(\phi_q - \phi_x)] \frac{c}{\omega} [i\beta_0(\omega) \cos \phi_q, i\beta_0(\omega) \sin \phi_q, -k_{\parallel}(\omega)] \\ &\times \frac{\omega}{c} \kappa_1(\omega) A_{\parallel}(k_{\parallel}(\omega) \cos \phi_q, k_{\parallel}(\omega) \sin \phi_q), \end{aligned} \quad (3.3)$$

where ϕ_q and ϕ_x are the azimuthal angles of the vectors \mathbf{q}_{\parallel} and \mathbf{x}_{\parallel} , respectively, measured from the x_1 axis. The total contribution from surface plasmon polaritons to the electric field in the vacuum in the region $x_1 > L/2$ is given by the sum of the expression given by Eq. (3.3) and the electric field of the incident surface plasmon polariton, which is given by the first term on the right-hand side of Eq. (2.4). It is this total field that is used in calculating the intensity distribution of the transmitted surface plasmon polariton field in the region $x_1 > L/2$.

Some preliminary results obtained from the preceding theory are presented in Fig 3.2. In Fig. 3.2(a) we present a color-level plot of the intensity distribution in this region when a surface plasmon polariton whose frequency $\omega = 2\pi c/\lambda$ corresponds to a vacuum wavelength $\lambda = 632.8\text{nm}$ has been transmitted through two slits of width $\Delta = 2\mu\text{m}$ that are separated by $d = 2\mu\text{m}$. The dielectric function $\epsilon_1(\omega) = -17.2$, while the dielectric function $\epsilon_2(\omega)$ has been given the value $\epsilon_2 = \infty$. Thus the slits are assumed to have perfectly conducting walls. The surface plasmon polariton beams emerging from the two slits spread with increasing distance from the exits of the slits. When the diffracted surface waves overlap an interference pattern is produced, whose signature is a central maximum. This is clearly seen in Fig. 3.2(b) where lateral cross sections of the intensity distribution at increasing distances from the exits of the slits are plotted, and show the evolution of the two-peaked intensity distribution close to the slits into a three-peaked distribution.

4. DISCUSSION AND CONCLUSIONS

In this work we have shown that a surface plasmon polariton beam incident on a straight boundary between two different metals with a common planar interface with vacuum produces a reflected surface plasmon polariton beam that is shifted along the boundary when its angle of incidence is greater than the critical angle for total internal reflection from that boundary. This is the analogue for surface plasmon polaritons of the Goos-Hänchen effect for volume electromagnetic waves. This result was obtained by the use of an impedance boundary condition at the vacuum-metal interface and a numerical solution of the integral equations for the amplitudes of the p - and s -polarized components of the electric field scattered by the boundary that arise from the use of this boundary condition.

The same approach was used to study the transmission of a surface plasmon polariton through a pair of slits fabricated on a planar, metal surface. It was shown that the transmitted electromagnetic field has a contribution from surface plasmon polaritons that has a distribution of intensity along a line perpendicular to the axes of the slits that displays the same kinds of diffraction and interference fringes as are observed in the intensity distribution of volume electromagnetic waves transmitted through a pair of nearby slits in an opaque screen. This is the analogue for surface plasmon polaritons of Young's double slit experiment.

Applications in which these properties of a surface plasmon can be exploited do not exist as yet. This study, therefore, is intended to add to the catalogue of properties of these surface electromagnetic waves some new ones, which might find their way into nanoscale devices some time in the future. They provide additional evidence that surface plasmon polaritons display the same diffraction and interference phenomena as do volume electromagnetic waves.

The methods we have used in obtaining these results, namely the numerical solution of two-dimensional integral equations, obtained through the use of impedance boundary conditions are well suited to the study of the kinds of problems considered here. They can be useful in studies of properties of surface plasmon polaritons on other kind of structured surfaces.

ACKNOWLEDGMENTS

This research was supported in part by AFRL contract AF 9453-08-C-0230.

REFERENCES

1. H. Shin and S. Fan, "All-angle negative refraction for surface plasmon waves using a metal-dielectric-metal structure," *Phys. Rev. Lett.* **96**, 073907(1-4) (2006).
2. H. J. Lezec, J. A. Dionne, and H. A. Atwater, "Negative refraction at visible frequencies," *Science* **316**, 430-432 (2007).
3. M. R. Dennis, N. I. Zheludev, and F. J. García de Abajo, "The plasmon Talbot effect," *Opt. Express* **15**, 9692-9700 (2007).
4. A. A. Maradudin and T. A. Leskova, "The Talbot effect for a surface plasmon polariton," *New J. Phys.* **11**, 033004 (1-9) (2009).
5. I. I. Smolyaninov, Y. J. Hung, and C. C. Davis, "Two-dimensional metamaterial structure exhibiting reduced visibility at 500 nm," *Opt. Lett.* **33** 1342-1344 (2008).
6. A. Tredicucci, C. Gmachl, F. Capasso, A. L. Hutchinson, D. L. Sivco, and A. Y. Cho, "Single-mode surface-plasmon laser," *Appl. Phys. Lett.* **76**, 2164-2166 (2000).
7. R. Li, A. Banerjee, and H. Grebel, "The possibility for surface plasmon lasers," *Opt. Express* **17**, 1622-1627 (2009).
8. R. Zia and M. L. Brongersma, "Surface plasmon polariton analogue to Young's double-slit experiment," *Nature Nanotechnology* **2**, 426-429 (2007).
9. F. Goos and H. Hänchen, "Ein neuer und fundamentaler Versuch zur Totalreflexion," *Ann. Phys.* **436** 333-346 (1947).
10. A. A. Maradudin, "The impedance boundary condition at a two-dimensional rough metal surface," *Opt. Commun.* **116**, 452-467 (1995).

11. T. Young, *A Course of Lectures on Natural Philosophy and the Mechanical Arts* (J. Johnson, London, 1807).
12. M. Born and E. Wolf, *Principles of Optics* 7th (expanded) edn. (Cambridge University Press, Cambridge, U.K., 2002), p. 297.
13. R. Zia, J. A. Schuller, and M. L. Brongersma, "Near-field characterization of guided polariton propagation and cutoff in surface plasmon waveguides," *Phys. Rev. B* **74**, 165415 (1-12) (2006).